VIP Electrocatalysis

DOI: 10.1002/ange.201303035

Electrochemical Synthesis of One-Dimensional Mesoporous Pt Nanorods Using the Assembly of Surfactant Micelles in Confined Space

*Cuiling Li, Takaaki Sato, and Yusuke Yamauchi**

One-dimensional metallic nanostructures, particularly those composed of noble metals, have sparked great scientific interest for practical applications, owing to their uniquely anisotropic structure.[1] Recent advances in energy conversion materials have shown that 1D materials are particularly effective as electrocatalysts for the methanol oxidation reaction (MOR) and oxygen reduction reaction (ORR) at low costs.[2] The facile synthesis of 1D Pt nanocatalysts (e.g., nanorods,[3] nanowires,[4] nanotubes,[5] and others[6]) with noteworthy enhanced electrocatalytic activity and durability is becoming increasingly important.

On the other hand, the formation of well-defined nano/mesoporous structures[7] of metals affords electrocatalysts showing a superior performance because of their high porosity, large area per unit volume, and excellent activity–structure relationship. Therefore, the successful synthesis of 1D mesoporous Pt motifs can be expected to be a new direction in the fabrication of superior electrocatalysts. The traditional hard-templating method, which is widely used to synthesize mesoporous carbon materials,[8] metal oxides,[9] and metals,[10] cannot easily be used for the synthesis of 1D mesoporous metal motifs, because this method involves several steps: the formation of an original template followed by deposition of metals within the mesopores and subsequent removal of the template. Lyotropic liquid crystals (LLCs) made of highly concentrated surfactants have also been used as soft templates.[11] However, due to the high viscosity of the LLCs, it is not so easy to deposit selectively metals in the target area. The method using LLCs cannot be applied as a general electrochemical method for shape-controlled synthesis of mesoporous metals. As another way, the alloy–dealloying approach, in which a less noble metal is selectively dissolved from a bimetallic alloy, is an attractive and much used strategy to synthesize porous metals.[12] However, it is hard to control the sizes of the mesopores and to construct robust mesopore walls.

Herein, we report a general "all-wet electrochemical approach" to synthesize novel self-supported 1D Pt nanorods (NRs) with a high density of mesopores (which are denoted as "mesoporous Pt nanorods, MPNRs") by using the assembly of micelles[13] in the confined space of a polycarbonate (PC) membrane. The MPNRs with various aspect ratios can be synthesized by simply controlling the electrodeposition times. The fabrication procedure of 1D MPNRs is schematically illustrated in Figure 1. A Pt thin film serving as conductive

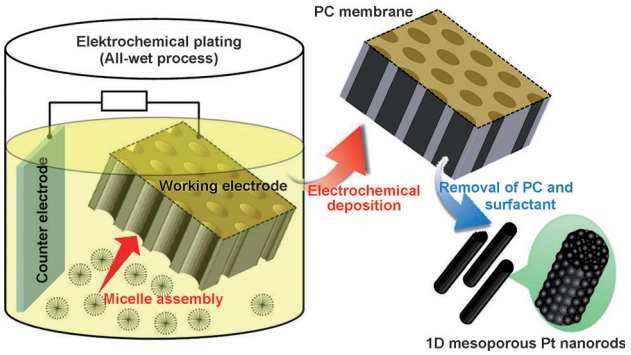

Figure 1. Electrochemical assembly of micelles in confined space for the preparation of 1D mesoporous Pt nanorods (MPNRs).

layer was deposited on one side of the PC membrane with a pore size of 50 nm (see Figure S1 in the Supporting Information). The electrolyte solution containing K_2PtCl_4 and 1.0 wt% Brij 58 ($C_{16}H_{33}(OCH_2CH_2)_{20}OH$) was used to prepare 1D MPNRs at a constant potential of −0.2 V vs. Ag/AgCl at room temperature. After the electrodeposition, the PC membranes were soaked in NaOH and ethanol solutions to dissolve the PC membranes and the surfactants, respectively.

Figure 2 displays the representative SEM images of the obtained 1D MPNRs. The obtained nanorods are straight and the mesopores are highly dispersed in each nanorod. The diameter of the obtained rods ranged from 50 to 120 nm, which was a little larger than the pore size of the channels of the original PC membranes. The same results were previously reported when PC filter membranes were used as templates to prepare 1D nanorods.[14] This is caused by the non-uniformity of the PC channels in the surface and the inner side. When the deposition time changed from 100 to 600 s, the lengths of the 1D MPNRs changed from 0.6 to 3.2 μm without any difference in the mesoporous structures (Figure S2), giving a growth speed of 5.3 nm s^{-1} (Figure S3; the measurements

[*] Dr. C. Li, Prof. Dr. Y. Yamauchi
World Premier International (WPI) Research Center for Materials Nanoarchitectonics (MANA)
National Institute for Materials Science (NIMS)
1-1 Namiki, Tsukuba, Ibaraki 305-0044 (Japan)
E-mail: Yamauchi.Yusuke@nims.go.jp
Homepage: http://www.yamauchi-labo.com
Prof. Dr. T. Sato
Shinshu University
Tokida 3-15-1, Ueda, Nagano 386-8567 (Japan)
Prof. Dr. Y. Yamauchi
Faculty of Science and Engineering, Waseda University
3-4-1 Okubo, Shinjuku, Tokyo 169-8555 (Japan)

Supporting information for this article is available on the WWW under http://dx.doi.org/10.1002/anie.201303035.

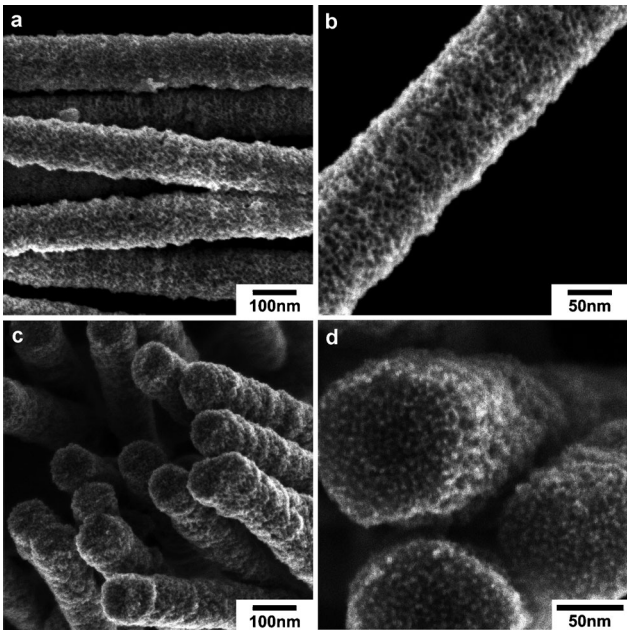

Figure 2. SEM images of the surface (a and b) and the cross-section (c and d; observed at edge part) of 1D MPNRs with length of 3.2 μm.

were also done at various times and the rate was established from these measurements.). All the data prove the successful preparation of 1D MPNRs with different aspect ratios.

Careful observation of the 1D MPNRs confirmed that there were lots of open mesopores all over the entire area (Figure 2). The size and wall thicknesses of the mesopores were statistically measured to be approximately 6–8 nm and 2–3 nm, respectively. A mesoporous structural feature was also clearly visualized by high-angle annular dark-field scanning TEM (HAADF-STEM; Figure S4). From the cross-sectional images (Figure 2c–d), it was clear that the mesoporous structures were well-developed even at the inner parts of the rods. Thus, the same mesoporous structure with uniform pore sizes was observed all over the rods, from bottom to top, from the surface to the inner side. Our MPNRs with open mesopores and thin wall thickness were well-assembled to be self-supported arrays (Figure S5). Such a successful formation of mesopores all over the entire rods can drastically increase the accessible specific surface area. As shown in Figure S4b, the *d* spacing (0.23 nm) for the adjacent fringes and the dihedral angle (70°) in the pore walls corresponded to the (111) planes of the Pt face-centered cubic (fcc) crystal structure. The selected-area electron diffraction (ED) patterns (Figure S4c) can be indexed as (111), (200), (220), and (311) planes of the Pt fcc crystal. The discrete diffraction spots indicate that the pore walls are composed of lots of nanosized Pt crystals. The broadening diffraction peaks of the wide-angle XRD profile (Figure S6) could be assigned to be Pt fcc crystals of a very small crystalline size, which was consistent with the TEM data (Figure S4c).

To investigate the micellar structure dissolved in the electrolyte, the solution inside the PC membrane was carefully characterized by small-angle X-ray scattering (SAXS; Figure S7). From the pair-distance distribution function ($p(r)$), the formation of spherical-like micelles formed in the electrolyte solution is confirmed (Figure S7a). As shown in Figure S7b, the maximum radius of the micelles in K_2PtCl_4 solution was about 6 nm, whereas that of the micelles in water was about 5 nm. The addition of Pt species induced a slight expansion of the micelles. The deduced $\Delta\rho(r)$ profiles further demonstrate that the electron density distributions with and without Pt species are almost perfectly identical up to a r value of about 4.0 nm from the center. The Pt species are distributed in the outermost shell between r values of about 4.0 and 6.0 nm. In the electrolyte solution, the dissolved Pt species are coordinated by water molecules to form metal–water complexes. The coordinated water molecules usually interact with ethylene oxide (EO) groups of the micelles, which has been studied by Dag et al.[15] Therefore, the dissolved $PtCl_4^{2-}$ ions adsorb inside the external EO region of the surfactant micelles. During the electrochemical deposition, the Pt species are thought to move to the working electrode together with the surfactant micelles.[13] Thus, the surfactant micelles dissolved in electrolyte solution can act as structural directing agents. From the SAXS study (Figure S7b), the mesopore size after Pt deposition can be estimated to be about 8 nm, which is almost identical to the average pore sizes in MPNRs observed in Figure 2 and Figure S2. As control experiments, in the absence of surfactant, 1D Pt nanorods without mesopores (hereafter abbreviated as PNRs) were obtained (Figure S8). On the other hand, when the concentration was over the critical micelle concentration (CMC), lots of mesopores had formed in the nanorods. Our method was applicable in a wide range of surfactant concentrations from 0.1 to 1.0 wt% (over CMC), in which the pore sizes were constant (Figure 2 and Figure S9). Consequently, 1D MPNRs are formed by confined Pt growth using electrochemical assembly of micelles.

The electrocatalytic performance of our self-supported 1D MPNRs toward the MOR was evaluated and compared with PNRs, mesoporous Pt NPs[16] (abbreviated as MPNPs, Figure S10), and commercially available Pt black (abbreviated as PtB). Two obvious anodic peaks, which are typical features of the methanol oxidation process, were observed on all the four samples during the positive and negative sweep in the cyclic voltammograms (Figure 3a). As three-dimensionally connected mesopores can make the entire surface readily accessible to reactants, our MPNRs demonstrated the highest mass-normalized current densities of 209 $mA\,mg^{-1}$ of Pt, which is around 2.4, 1.4, and 2.8 times higher than that of PNRs (87.6 $mA\,mg^{-1}$ of Pt), MPNPs (152 $mA\,mg^{-1}$ of Pt), and PtB (75.6 $mA\,mg^{-1}$ of Pt). The mass activity of our MPNRs was also higher than that of state-of-art Pt-based nanomaterials reported previously, such as nanoporous Pt-Co alloy nanowires,[12a] single-crystal Pt nanowires on a Sn@CNT nanocable (PtNW-Sn@CNTs), commercial ETEK Pt/C catalyst (30 wt% Pt),[17] Pt nanoparticles loaded on PBI-MWCNTs (MWCNT/PBI/Pt),[18] and Pt nanoparticles assembled in a poly(ethylenimine) matrix (PEI/Pt NP)[19]. (All measurements found in the literature were done in 0.5 M methanol.) The value of I_f/I_b (defined as the ratio between the forward and backward current densities) can be used as an

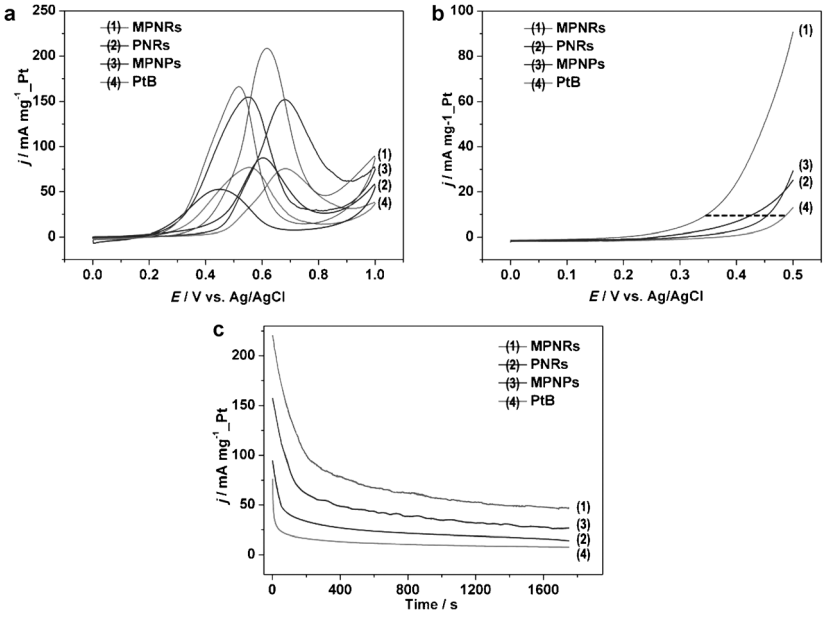

Figure 3. a) Cyclic voltammograms, b) linear-sweep voltammograms, and c) chronoamperometric curves (recorded at 0.6 V) for methanol oxidation reactions catalyzed by MPNRs (1), PNRs (2), MPNPs (3), and PtB (4), respectively, in 0.1 M $HClO_4$ solution containing 0.5 M methanol. The current densities (*Y* axis) are normalized by the mass of Pt (mg).

indicator of the CO-tolerance of Pt catalysts in the MOR. The I_f/I_b values were 1.25, 1.66, 0.99, and 0.98 for MPNRs, PNRs, MPNPs, and PtB, respectively. The higher I_f/I_b value of 1D MPNRs indicates its relatively good poison tolerance.[20] Furthermore, our 1D self-supported MPNRs and PNRs showed a remarkably negatively shifted peak potential and onset potential for the electrocatalytic oxidation of methanol in comparison with MPNPs and PtB catalysts (known as 0D nanostructures; Figure 3b). Chronoamperometry, a useful method for the evaluation as electrocatalysts, was employed to investigate the electrochemical performance of MPNRs (Figure 3c). All the data nicely shows that the integration of 1D and mesoporous structures can guarantee a good catalytic performance toward the oxidation of methanol.

The electrocatalytic activity of 1D MPNRs for the ORR was also investigated (Figure S11). The half-wave potential of self-supported 1D MPNRs (0.78 V) was equal to that of PNRs (0.78 V), and was higher than those of MPNPs (0.77 V), and PtB (0.74 V), indicating that 1D structured Pt motifs were superior in the electrocatalytic ORR. Figure S11b compares the currents of four catalysts at 0.80 V, normalized by Pt mass (mass activity) and Pt electrochemically active surface area (ECSA) (specific activity). The mass activity of 1D MPNRs was about 11.5 $A\,g^{-1}$ of Pt, which was 1.8, 1.7, and 2.9 times higher than that of PNRs (6.54 $A\,g^{-1}$ of Pt), MPNPs (6.82 $A\,g^{-1}$ of Pt), and PtB (3.92 $A\,g^{-1}$ of Pt), respectively, indicating that the mesoporous architecture in the Pt nanorods can highly improve the utilization efficiency of Pt in the electro-reduction of oxygen. The polarization curves of a MPNRs-modified glassy carbon rotating disk electrode (GC RDE) were recorded at different rotation rates. The expected increase of the limiting diffusion current density was observed as a function of the rotation rate (Figure S11c). The corresponding Koutecky–Levich (K-L) plots showed the first-order reaction kinetics toward the dissolved O_2 on MPNRs from 0.3 to 0.6 V (Figure S11d).[21] The calculated number of transferred electrons during the reduction of oxygen was between 4.03–4.18, thereby indicating that the ORR from 0.3 to 0.6 V was dominated by a four-electron ($4e^-$) process and O_2 was reduced to OH^-.

Furthermore, we investigated the durability of the electrocatalysts under harsh cycling treatment. The initial ECSAs of MPNRs, PNRs, MPNPs, and PtB were determined from the cyclic voltammetry (CV) curves of these four catalysts recorded in 0.1 M $HClO_4$ solutions at a sweep rate of 50 $mV\,s^{-1}$ (Figure S12). The specific ECSA of MPNRs showed a reasonably high surface area (46.2 $m^2\,g^{-1}$ of Pt), which was equal to that of MPNPs (48.5 $m^2\,g^{-1}$ of Pt). The CV curves of four catalysts after 50–2000 cycles were recorded for harsh accelerated durability tests with the cyclic potential sweeping between −0.2 and 1.0 V (Figure S13). The current densities of the peaks in hydrogen adsorption/desorption potential region for the MPNPs dropped dramatically with the increase of the number of CV cycles (Figure S13c), although the original ECSA before the CV cycles showed a value similar to that of MPNRs (Figure S12b). The drastic loss of the ECSA was also observed for the PtB catalyst (Figure S13d). In contrast, the 1D MPNRs and PNRs exhibited only a slight drop in the current densities of the peaks upon cycling in the same potential range. After careful calculation, the loss of ECSAs with cycling was plotted in Figure S13e. After 1000 cycles, the self-supported 1D MPNRs lost only 25% of the initial Pt ECSA, while the PtB and MPNPs catalysts lost most of their initial ECSAs. Even when the durability test for self-supported 1D MPNRs was further prolonged to 2000 cycles, the Pt ECSA dropped only 31%. This result demonstrates that 1D MPNRs have a significantly high stability.

In summary, we successfully designed self-supported 1D MPNRs by an all-wet electrochemical synthesis inside the confined space of a PC membrane. The mesoporous structures with a 6–8 nm pore size and a thin wall thickness were well-developed all over the rod surface and inside Pt NRs. The 1D motifs exhibited high activity and CO-tolerant performance in the electro-oxidation of methanol, and our MPNRs showed only 31% loss of ESCA even after a harsh accelerated durability test. Thus, the self-supported mesoporous structures are highly desired in high activity and stability for the large surface area with less aggregation and ripening of Pt nanoparticles.[21] The 1D geometry can maintain improved electron transport characteristics because of the path-directing effects of the structural anisotropy.[2] Also, the mesoporous structures with connected thin walls can provide facile pathways for electron and mass transfer by reducing the interface resistance. This work demonstrates that the self-supported, 1D, and mesoporous structures are indeed prom-

ising architectures to highly improve the catalytic activity and durability of catalysts for the MOR. Such geometrically favorable factors will provide a new avenue in designing highly efficient electrocatalysts used in artificial energy conversion systems.

Received: April 11, 2013
Published online: June 26, 2013

Keywords: electrochemistry · mesoporous materials · micelles · nanorods · platinum

[1] a) C. Gao, Q. Zhang, Z. Lu, Y. Yin, *J. Am. Chem. Soc.* **2011**, *133*, 19706 – 19709; b) C. Koenigsmann, E. Sutter, T. A. Chiesa, R. R. Adzic, S. S. Wong, *Nano Lett.* **2012**, *12*, 2013 – 2020; c) Z. Chen, M. Waje, W. Li, Y. Yan, *Angew. Chem.* **2007**, *119*, 4138 – 4141; *Angew. Chem. Int. Ed.* **2007**, *46*, 4060 – 4063; d) H.-W. Liang, S. Liu, J.-Y. Gong, S.-B. Wang, L. Wang, S.-H. Yu, *Adv. Mater.* **2009**, *21*, 1850 – 1854.

[2] a) S. Guo, S. Zhang, X. Sun, S. Sun, *J. Am. Chem. Soc.* **2011**, *133*, 15354 – 15357; b) M. Mohl, A. Kumar, A. L. M. Reddy, A. Kukovecz, Z. Konya, I. Kiricsi, R. Vajtai, P. M. Ajayan, *J. Phys. Chem. C* **2010**, *114*, 389 – 393; c) H.-W. Liang, X. Cao, F. Zhou, C.-H. Cui, W.-J. Zhang, S.-H. Yu, *Adv. Mater.* **2011**, *23*, 1467 – 1471.

[3] a) S.-H. Yoo, S. Park, *Adv. Mater.* **2007**, *19*, 1612 – 1615; b) F. Liu, J. Y. Lee, W. J. Zhou, *Small* **2006**, *2*, 121 – 128; c) K. D. Osberg, A. L. Schmucker, A. J. Senesi, C. A. Mirkin, *Nano Lett.* **2011**, *11*, 820 – 824.

[4] a) X. Zhang, W. Lu, J. Da, H. Wang, D. Zhao, P. A. Webley, *Chem. Commun.* **2009**, 195 – 197; b) J. M. Kim, H. I. Joh, S. M. Jo, D. J. Ahn, H. Y. Ha, S. A. Hong, S.-K. Kim, *Electrochim. Acta* **2010**, *55*, 4827 – 4835.

[5] a) Y. Luo, S. K. Lee, H. Hofmeister, M. Steinhart, U. Gösele, *Nano Lett.* **2004**, *4*, 143 – 147; b) L. X. Ding, G. R. Li, Z. L. Wang, Z. Q. Liu, H. Liu, Y. X. Tong, *Chem. Eur. J.* **2012**, *18*, 8386 – 8391; c) S. M. Alia, G. Zhang, D. Kisailus, D. Li, S. Gu, K. Jensen, Y. Yan, *Adv. Funct. Mater.* **2010**, *20*, 3742 – 3746.

[6] a) M. L. Lin, C. C. Huang, M. Y. Lo, C. Y. Mou, *J. Phys. Chem. C* **2008**, *112*, 867 – 873; b) B. Lim, M. Jiang, P. H. C. Camargo, E. C. Cho, J. Tao, X. Lu, Y. Zhu, Y. Xia, *Science* **2009**, *324*, 1302 – 1305; c) B. H. Wu, N. F. Zheng, G. Fu, *Chem. Commun.* **2011**, *47*, 1039 – 1041; d) M. Chen, B. H. Wu, J. Yang, N. F. Zheng, *Adv. Mater.* **2012**, *24*, 862 – 879; e) G. X. Chen, Y. M. Tan, B. H. Wu, G. Fu, N. F. Zheng, *Chem. Commun.* **2012**, *48*, 2758 – 2760.

[7] a) C. P. Tsai, Y. Hung, Y. H. Chou, D. M. Huang, J. K. Hsiao, C. Chang, Y. C. Chen, C. Y. Mou, *Small* **2008**, *4*, 186 – 191; b) H. M. Liu, S. H. Wu, C. W. Lu, M. Yao, J. K. Hsiao, Y. Hung, Y. S. Lin, C. Y. Mou, C. S. Yang, D. M. Huang, Y. C. Chen, *Small* **2008**, *4*, 619 – 626; c) J. Liu, S. Z. Qiao, Q. H. Hu, G. Q. Lu, *Small* **2011**, *7*, 425 – 443; d) J. Liu, S. B. Hartono, Y. G. Jin, Z. Li, G. Q. Lu, S. Z. Qiao, *J. Mater. Chem.* **2010**, *20*, 4595 – 4601.

[8] a) T. W. Kim, I. S. Park, R. Ryoo, *Angew. Chem.* **2003**, *115*, 4511 – 4515; *Angew. Chem. Int. Ed.* **2003**, *42*, 4375 – 4379; b) S. H. Joo, S. J. Choi, I. Oh, J. Kwak, Z. Liu, O. Terasaki, R. Ryoo, *Nature* **2001**, *412*, 169 – 172; c) A. H. Lu, W. Schmidt, A. Taguchi, B. Spliethoff, B. Tesche, F. Schüth, *Angew. Chem.* **2002**, *114*, 3639 – 3642; *Angew. Chem. Int. Ed.* **2002**, *41*, 3489 – 3492.

[9] a) Z. X. Wu, Q. Li, D. Feng, P. A. Webley, D. Zhao, *J. Am. Chem. Soc.* **2010**, *132*, 12042 – 12050; b) C. Dickinson, W. Zhou, R. P. Hodgkins, Y. Shi, D. Zhao, H. He, *Chem. Mater.* **2006**, *18*, 3088 – 3095; c) A. H. Lu, F. Schüth, *Adv. Mater.* **2006**, *18*, 1793 – 1805.

[10] a) Y. Wu, G. Cheng, K. Katsov, S. W. Sides, J. Wang, J. Tang, G. H. Fredrickson, M. Moskovits, G. D. Stucky, *Nat. Mater.* **2004**, *3*, 816 – 822; b) D. Wang, H. Luo, R. Kou, M. P. Gil, S. Xiao, V. O. Golub, Z. Yang, C. J. Brinker, Y. Lu, *Angew. Chem.* **2004**, *116*, 6295 – 6299; *Angew. Chem. Int. Ed.* **2004**, *43*, 6169 – 6173; c) H. Wang, H. Y. Jeong, M. Imura, L. Wang, L. Radhakrishnan, N. Fujita, T. Castle, O. Terasaki, Y. Yamauchi, *J. Am. Chem. Soc.* **2011**, *133*, 14526 – 14529.

[11] a) G. S. Attard, C. G. Göltner, J. M. Corker, S. Henke, R. H. Templer, *Angew. Chem.* **1997**, *109*, 1372 – 1374; *Angew. Chem. Int. Ed. Engl.* **1997**, *36*, 1315 – 1317; b) G. S. Attard, S. A. A. Leclerc, S. Maniguet, A. E. Russell, I. Nandhakumar, P. N. Bartlett, *Chem. Mater.* **2001**, *13*, 1444 – 1446; c) Y. Yamauchi, K. Kuroda, *Chem. Asian J.* **2008**, *3*, 664 – 676; d) Y. Yamauchi, A. Sugiyama, R. Morimoto, A. Takai, K. Kuroda, *Angew. Chem.* **2008**, *120*, 5451 – 5453; *Angew. Chem. Int. Ed.* **2008**, *47*, 5371 – 5373; e) Y. Yamauchi, A. Tonegawa, M. Komatsu, H. Wang, L. Wang, Y. Nemoto, N. Suzuki, K. Kuroda, *J. Am. Chem. Soc.* **2012**, *134*, 5100 – 5109; f) X. Zhang, W. Lu, J. Dai, L. Bourgeois, N. Hao, H. Wang, D. Zhao, P. A. Webley, *Angew. Chem.* **2010**, *122*, 10299 – 10303; *Angew. Chem. Int. Ed.* **2010**, *49*, 10101 – 10105.

[12] a) L. Liu, E. Pippel, R. Scholz, U. Gösele, *Nano Lett.* **2009**, *9*, 4352 – 4358; b) J. I. Shui, C. Chen, J. C. M. Li, *Adv. Funct. Mater.* **2011**, *21*, 3357 – 3362; c) C. Zhu, S. Guo, S. Dong, *Adv. Mater.* **2012**, *24*, 2326 – 2331; d) S. Tominaka, T. Hayashi, Y. Nakamura, T. Osaka, *J. Mater. Chem.* **2010**, *20*, 7175 – 7182.

[13] H. Wang, L. Wang, T. Sato, Y. Sakamoto, S. Tominaka, K. Miyasaka, N. Miyamoto, Y. Nemoto, O. Terasaki, Y. Yamauchi, *Chem. Mater.* **2012**, *24*, 1591 – 1598.

[14] a) N. Suzuki, T. Kimura, Y. Yamauchi, *J. Mater. Chem.* **2010**, *20*, 5294 – 5300; b) H. Zhou, S. S. Wong, *ACS Nano* **2008**, *2*, 944 – 958.

[15] a) Ö. Çelik, Ö. Dag, *Angew. Chem.* **2001**, *113*, 3915 – 3919; *Angew. Chem. Int. Ed.* **2001**, *40*, 3799 – 3803; b) A. F. Demirörs, B. E. Eser, Ö. Dag, *Langmuir* **2005**, *21*, 4156 – 4162; c) Ö. Dag, S. Alayoğlu, İ. Uysal, *J. Phys. Chem. B* **2004**, *108*, 8439 – 8446.

[16] a) L. Wang, M. Imura, Y. Yamauchi, *ACS Appl. Mater. Interfaces* **2012**, *4*, 2865 – 2869; b) L. Wang, Y. Yamauchi, *Chem. Eur. J.* **2011**, *17*, 8810 – 8815.

[17] S. Sun, G. Zhang, D. Geng, Y. Chen, M. N. Banis, R. Li, M. Cai, X. Sun, *Chem. Eur. J.* **2010**, *16*, 829 – 835.

[18] M. Okamoto, T. Fujigaya, N. Nakashima, *Small* **2009**, *5*, 735 – 740.

[19] L. Bai, H. Zhu, J. S. Thrasher, S. C. Street, *ACS Appl. Mater. Interfaces* **2009**, *1*, 2304 – 2311.

[20] a) C. Li, Y. Yamauchi, *Phys. Chem. Chem. Phys.* **2013**, *15*, 3490 – 3496; b) M. Cao, D. Wu, S. Gao, R. Cao, *Chem. Eur. J.* **2012**, *18*, 12978 – 12985.

[21] a) S. Guo, S. Sun, *J. Am. Chem. Soc.* **2012**, *134*, 2492 – 2495; b) Y. Zhang, K. Fugane, T. Mori, L. Niu, J. Ye, *J. Mater. Chem.* **2012**, *22*, 6575 – 6580; c) D. Wang, H. L. Xin, H. Wang, Y. Yu, E. Rus, D. A. Muller, F. J. DiSalvo, H. D. Abruña, *Chem. Mater.* **2012**, *24*, 2274 – 2281.

